

Gas depletion in cluster galaxies depends strongly on their internal structure

Wei Zhang^{1*}, Cheng Li², Guinevere Kauffmann³, Ting Xiao^{2†}

¹ *National Astronomical Observatories, Chinese Academy of Sciences, 20A Datun Road, Chaoyang District, Beijing 100012, China*

² *Partner Group of Max Planck Institut for Astrophysics and Key Laboratory for Research in Galaxies and Cosmology of Chinese Academy of Sciences, Shanghai Astronomical Observatory, Nandan Road 80, Shanghai 200030, China*

³ *Max Planck Institut für Astrophysik, Karl-Schwarzschild-Strasse 1, 85748 Garching, Germany*

Accepted Received; in original form

ABSTRACT

We analyze galaxies in 300 nearby groups and clusters identified in the Sloan Digital Sky Survey using a photometric gas mass indicator that is useful for estimating the degree to which the interstellar medium of a cluster galaxy has been depleted. We study the radial dependence of inferred gas mass fractions for galaxies of different stellar masses and stellar surface densities. At fixed clustercentric distance and at fixed stellar mass, lower density galaxies are more strongly depleted of their gas than higher density galaxies. An analysis of depletion trends in the two-dimensional plane of stellar mass M_* and stellar mass surface density μ_* reveals that gas depletion at fixed clustercentric radius is much more sensitive to the density of a galaxy than to its mass. We suggest that low density galaxies are more easily depleted of their gas, because they are more easily affected by ram-pressure and/or tidal forces. We also look at the dependence of our gas fraction/radius relations on the velocity dispersion of the cluster, finding no clear systematic trend.

Key words: galaxies: clusters: general – galaxies: distances and redshifts.

1 INTRODUCTION

The observed variation in galaxy colours, star formation rates, cold gas fractions as a function of distance from the centers of groups and clusters places important constraints on the physical processes that affect the gas in galaxies as they evolve within a hierarchy of merging dark matter halos (e.g. Diaferio et al. 2001; Okamoto & Nagashima 2003).

Semi-analytic models of galaxy formation developed in the early 1990’s (e.g. Kauffmann et al. 1993; Cole et al. 1994) made the simplistic assumption that after a galaxy was accreted by a larger dark matter halo and became a satellite, its reservoir of hot gas would be stripped instantaneously and would form part of the hot atmosphere bound to the common halo. It was also assumed that the cold gas in a galaxy was not affected by stripping processes and the timescale for the satellite galaxy to redden was set by the rate at which the cold gas was used up by star formation. Comparison of these models with group and cluster galaxies from the Sloan Digital Sky Survey revealed that the predicted fraction of blue satellite galaxies was too low (Weinmann et al. 2006). This discovery was then followed by

considerable effort to fix the models by relaxing the assumption that the hot gas reservoir around a satellite is stripped instantaneously following accretion (e.g. Font et al. 2008; Weinmann et al. 2010; Guo et al. 2011). If satellite galaxies are able to retain a significant fraction of their hot gas for several gigayears following accretion, their colours are found to be in much better agreement with data.

One important constraint from the observations that has not been considered in much detail up to now, is the fact that the increase in the fraction of red galaxies from the outskirts of rich groups and clusters to their centers, is strongly dependent on galaxy mass. As shown in Figure 7 of von der Linden et al. (2010), the fraction of red galaxies with stellar masses in the range $3 \times 10^9 M_\odot$ to $10^{10} M_\odot$ increases by a factor 4 from 0.2 at the virial radius of the cluster to 0.8 at the cluster center. In contrast, for galaxies with stellar masses greater than $5 \times 10^{10} M_\odot$, the red fraction only increases by 30% from 0.6 at the virial radius to 0.8 at the cluster center. Because cold gas consumption times in low mass field galaxies are long, one might ask whether stripping of an external reservoir of ionized or hot gas can lead to such strong effects with cluster-centric radius. In a recent paper, Guo et al. (2011) implemented a model in which the hot gas mass around satellites is reduced in direct proportion to the mass of its surrounding dark matter subhalo, which loses

* E-mail:xtwfn@bao.ac.cn

† LAMOST fellow

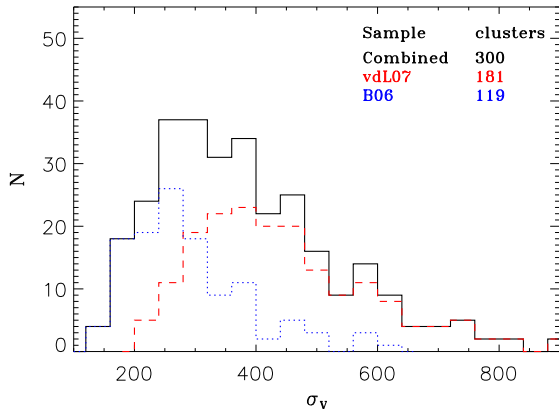


Figure 1. Histograms of the velocity dispersion σ_V of the clusters in our sample. The black solid histogram is for the full sample, while the red dashed and blue dotted histograms are for the subsets from von der Linden et al. (2007) and Berlind et al. (2006).

mass continuously due to tidal stripping. In addition, Guo et al computed the radius at which ram-pressure forces due to the satellite’s motion through the intracluster medium would remove the hot gas. The minimum of the tidal radius and the ram-pressure stripping radius define the radius beyond which gas is removed from the subhalo. As shown in their Figure 2, this model does not reproduce the stellar mass dependence of cluster galaxy red fractions at distances less than $\sim 0.5R_{vir}$ from the cluster center.

In this paper, we analyze 300 clusters and groups from the samples of Berlind et al. (2006) and von der Linden et al. (2007), looking for clues as to why environmental effects on low mass galaxies are so dramatic. In section 2, we describe the cluster and galaxy samples and introduce a photometric gas mass indicator that is useful for estimating the degree to which the interstellar medium of a cluster galaxy has been depleted with respect to a similar galaxy in the field. In section 3, we study the radial dependence galaxy colours/gas fractions in the two-dimensional plane of stellar mass M_* and stellar mass surface density μ_* . At fixed cluster-centric radius, we find that decrease in inferred cold gas mass fraction is a stronger function of stellar surface mass density than stellar mass. In section 4, we look at the dependence of stripping effects on the cluster/group velocity dispersion and in section 5, we summarize and discuss the implications of our results. Throughout this paper we assume a spatially flat concordance cosmology with $\Omega_m = 0.3$, $\Omega_\Lambda = 0.7$ and $H_0 = 100h \text{ km s}^{-1} \text{ Mpc}^{-1}$, where $h = 0.7$.

2 DATA

2.1 The cluster catalogue

The cluster catalogue used in this paper includes 300 unique galaxy clusters, of which 181 were identified by von der Linden et al. (2007, hereafter vdL07) from the SDSS data release 4 (DR4) and 119 were identified by Berlind et al. (2006, hereafter B06) from an earlier SDSS

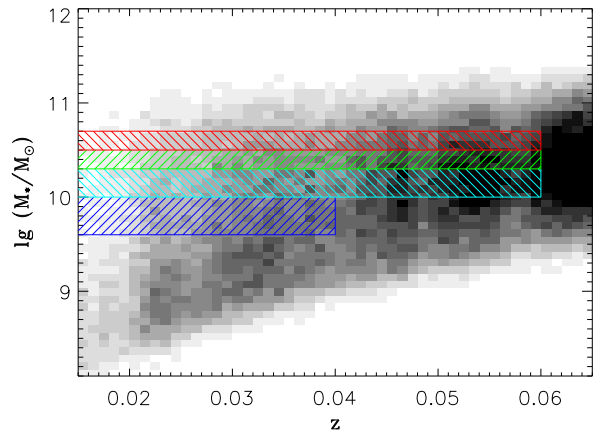


Figure 2. The shaded contours show the distribution of parent sample galaxies in the plane of stellar mass versus redshift. The four coloured boxes indicate the redshifts limits of the four stellar mass sub-samples analyzed in this paper.

data release (DR3). Our cluster sample is restricted to have redshift $z < 0.06$ (see next section), to have richness $N_{member} \geq 10$, velocity dispersion $\sigma_V \geq 150 \text{ km s}^{-1}$ and area completeness $f_{cover} \geq 0.5$. The area completeness is defined by

$$f_{cover} = \frac{A_{survey}(< 2r_{200})}{A_{full}(< 2r_{200})}, \quad (1)$$

where $A_{full}(< 2r_{200})$ is a circular sky area centered on the brightest cluster galaxy (BCG) with radius twice the virial radius of the cluster (r_{200}), and A_{survey} is the area inside the same circle that is covered by the SDSS survey. The area completeness is unity for clusters far enough from the survey edges, but can be very low for clusters near the edges. Following Finn et al. (2005), we estimate a virial radius for each of our clusters, r_{200} as

$$r_{200} = \frac{\sigma_V}{1000 \text{ km s}^{-1}} \frac{1}{\sqrt{\Omega_\Lambda + \Omega_m(1+z)^3}} h^{-1} \text{ Mpc}. \quad (2)$$

In Figure 1 we show a histogram of σ_V for the cluster sample. We note that the vdL07 sample is actually a subset of clusters in the C4 catalogue of Miller et al. (2005), who identified clusters based on the presence of a “red sequence” of galaxies with similar positions and redshifts. vdL07 implemented an improved method for identifying the brightest cluster galaxy (BCG) and recalculated the velocity dispersion for each cluster accordingly. The cluster-finding algorithm of B06 was based on a redshift-space friends-of-friends method with no requirement that there be a clearly defined red sequence. As can be seen from the figure, the clusters from vdL07 have higher velocity dispersions than the clusters from B06. The combination of the two gives a sample with a wide coverage of velocity dispersion, ranging from $\sim 150 \text{ km/s}$ to $\sim 800 \text{ km/s}$. This corresponds to a wide range in dark matter halo mass, from $M_h \sim 2 \times 10^{12} M_\odot$ for the Milky Way-type halos up to $M_h \sim 5 \times 10^{14} M_\odot$ for the most massive halos in the local Universe (see e.g. Li et al. 2012a).

In this paper, we show results only for the combined sample of clusters. We have tested that all conclusions presented in this paper hold when we analyze the vdL07 and

Table 1. Volume-limited samples selected by stellar mass from the SDSS/DR7 galaxy sample

Sample	Stellar mass	Redshift	N_{gal}
M1	$9.60 < \log(M_*/M_\odot) < 10.0$	$z < 0.04$	4169
M2	$10.0 < \log(M_*/M_\odot) < 10.3$	$z < 0.06$	9004
M3	$10.3 < \log(M_*/M_\odot) < 10.5$	$z < 0.06$	5577
M4	$10.5 < \log(M_*/M_\odot) < 10.7$	$z < 0.06$	4763

B06 cluster samples separately. The quantitative relations between HI gas mass fraction and cluster-centric radius in bins of stellar mass and stellar surface density agree for the two samples within the statistical errors. Combining the samples allows us to test whether there are any clear differences in galaxy properties at fixed r/r_{200} for clusters with low and high velocity dispersions. As we will show in Section 4, these differences are very small.

2.2 The galaxy sample

We begin with the parent galaxy sample constructed from the New York University Value Added Catalogue (NYU-VAGC) **sample dr72** (Blanton et al. 2005), which consists of about half a million galaxies with $r < 17.6$, $-24 < M_{0.1,r} < -16$ and redshifts in the range $0.01 < z < 0.5$. Here, r is the r -band Petrosian apparent magnitude, corrected for Galactic extinction, and $M_{0.1,r}$ is the r -band Petrosian absolute magnitude, corrected for evolution and K -corrected to its value at $z = 0.1$.

From the parent sample, we select four volume-limited samples of galaxies according to their stellar mass and redshift. The stellar mass range, the redshift range and the number of galaxies of the samples are listed in Table 1. The four volume-limited samples include a total of 23,513 galaxies. In Figure 2 we indicate the selection criteria of our samples in the stellar mass versus redshift plane. The parent sample is plotted in the background, grey-coded by the number of galaxies. The samples we choose are the same as in von der Linden et al. (2010, hereafter vdL10; see the left-hand panel of their fig.5), except that we impose an upper redshift cut at $z = 0.06$.

2.3 HI mass fraction and HI deficiency

When discussing the effect of the cluster environment on galaxies, it is much more physically intuitive to carry out analyses using *cold gas mass fractions* rather than colours or star formation rates. This is because we are trying to understand the impact of processes such as ram-pressure or tidal stripping on the interstellar medium of galaxies.

In recent years, ‘pseudo’ HI gas mass estimates have been introduced that rely on the fact that the HI gas mass fraction is strongly correlated with properties such optical and optical/IR colours (e.g. Kannappan 2004). Subsequent studies established that a combination of colour and stellar surface mass density provides a more accurate estimation of the HI mass fraction (e.g. Zhang et al. 2009; Catinella et al. 2010; Li et al. 2012b).

The most recent version of such estimators was pro-

posed by Li et al. (2012b, hereafter L12) and utilizes a combination of four galaxy parameters:

$$\log(M_{\text{HI}}/M_*) = -0.325 \log \mu_* - 0.237(NUV - r) - 0.354 \log M_* - 0.513 \Delta_{g-i} + 6.504, (3)$$

M_* is the stellar mass; μ_* is the surface stellar mass density given by $\log \mu_* = \log M_* - \log(2\pi R_{50}^2)$ (R_{50} is the radius enclosing half the total z -band Petrosian flux and is in units of kpc). $NUV - r$ is the global near-ultraviolet (NUV) to r -band colour. The NUV magnitude is provided by the GALEX pipeline and the $NUV - r$ colour is corrected for Galactic extinction following Wyder et al. (2007) with $A_{NUV-r} = 1.9807 A_r$, where A_r is the extinction in r -band derived from the dust maps of Schlegel et al. (1998). Δ_{g-i} is the colour gradient defined as the difference in $g - i$ colour between the outer and inner regions of the galaxy. The inner region is defined to be the region within R_{50} and the outer region is the region between R_{50} and R_{90} . The estimator has been calibrated using samples of nearby galaxies ($0.025 < z < 0.05$) with HI line detections from the GALEX Arecibo SDSS Survey (GASS; Catinella et al. 2010), and is demonstrated to provide unbiased HI-to-stellar mass ratio estimates, M_{HI}/M_* , even for HI-rich galaxies.

As well as the HI mass fraction, we will also work with an ‘HI deficiency parameter’, H_{def} which we define as the deviation in $\log(M_{\text{HI}}/M_*)$ from the value predicted from the mean relation between $\log(M_{\text{HI}}/M_*)$ and galaxy mass M_* and stellar surface mass density μ_* (see Li et al. 2012b):

$$H_{def} = \log(M_{\text{HI}}/M_*) - \log(M_{\text{HI}}/M_*)|(M_*, \mu_*) \quad (4)$$

where $\log(M_{\text{HI}}/M_*)$ is estimated by equation (3) and

$$\log(M_{\text{HI}}/M_*)|(M_*, \mu_*) = -0.227 \log M_* - 0.646 \log \mu_* + 7.166. (5)$$

The relation between the stellar mass of a galaxy and its structural parameters such as stellar surface mass density and concentration index have been found to depend extremely weakly on environment (e.g. Kauffmann et al. 2004; Weinmann et al. 2009). The HI deficiency parameter is thus the most direct measure of the degree to which gas has been depleted in a given cluster galaxy.

Because the photometric estimator in equation (3) has been calibrated using the GASS sample, one might question whether it is still valid for galaxies in cluster environments. Cortese et al. (2011) used a sample of ~ 300 nearby galaxies to investigate the effect of the environment on HI scaling relations and found that Virgo cluster galaxies still lie on the same ‘plane’ relating HI gas mass fraction to stellar surface mass density and colour, even though they are significantly offset towards lower gas content compared to field galaxies.

In Figure 3 we use ~ 8000 galaxies from the Arecibo Legacy Fast ALFA survey (ALFALFA; Giovanelli et al. 2005) to test whether L12 estimator exhibits any significant environmental dependence. We plot the residual in the estimated HI mass fraction, defined as the difference between the estimated $\log(M_{\text{HI}}/M_*)$ value and the observed value, as a function of overdensity, $\ln(1 + \delta)$. The overdensity parameter, δ has been estimated by Jasche et al. (2010) through reconstruction of the 3D density field from the SDSS DR7 data. In the right-hand panel of the same figure we plot the histograms of the residual for subsets of galaxies selected by $\ln(1 + \delta)$. We find that the residual in the estimated HI mass fraction exhibits a weak, but systematic trend with

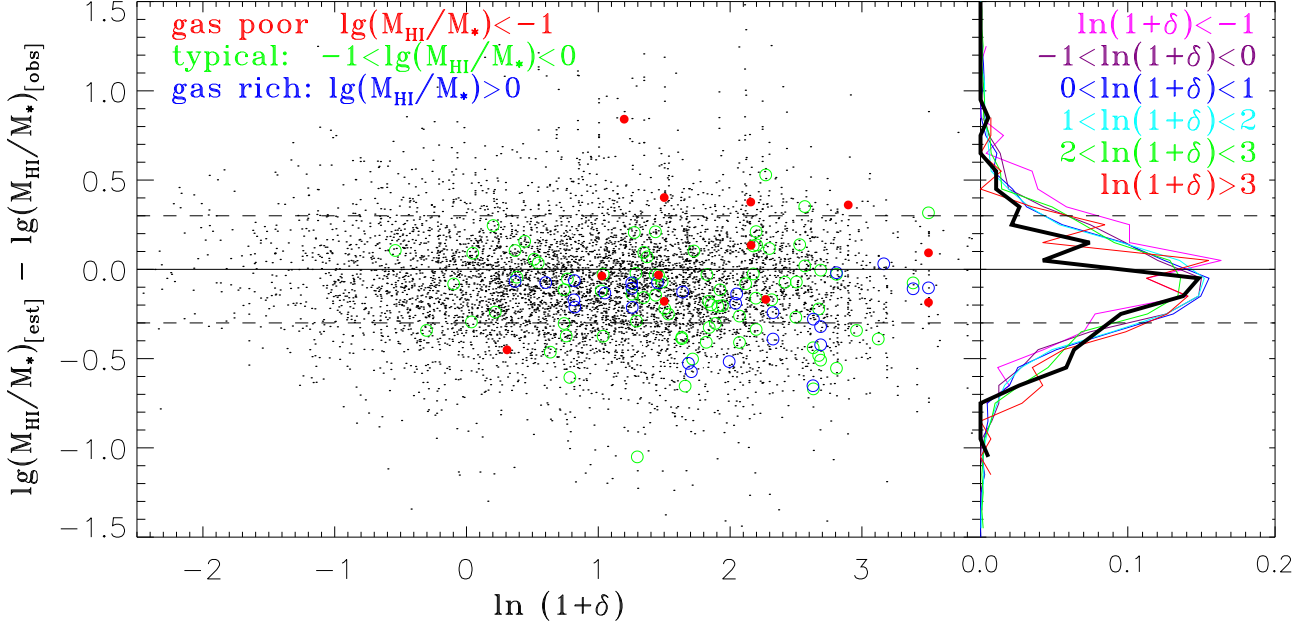


Figure 3. The residual in the estimated HI mass fraction, defined as the difference between the estimated $\lg(M_{\text{HI}}/M_*)$ value and the observed value, is plotted as a function of overdensity, $\ln(1+\delta)$. In the left panel, the black points are SDSS galaxies detected by ALFALFA. The red, green and blue circles are group/cluster galaxies identified by Berlind et al. (2006) that have been detected by ALFALFA. Red symbols show “gas poor” cluster galaxies, green symbols show “typical” cluster galaxies and blue symbols indicate “gas rich” cluster galaxies, with HI mass fractions as indicated on the plot. In the right panel, the ALFALFA galaxies have been separated into six subsamples according to local density, as indicated on top of the panel. The distributions of gas fraction residuals of these subsamples are shown as coloured lines. The distribution of gas fraction residuals of the B06 cluster galaxies is shown as a thick solid black line.

overdensity, in the sense that the gas fractions of galaxies in high-density regions are slightly underestimated. Cluster galaxies detected by ALFALFA that are included in the B06 group/cluster catalogue are plotted as coloured symbols in Figure 3 and the distribution of residuals is shown as a solid black line in the right hand panel. As can be seen, the HI content of cluster galaxies is underestimated by 0.1 dex on average, but the galaxies that cause this shift are the *gas-rich* rather than the *gas-poor* group/cluster members. This particular paper is focused on the physical processes that cause galaxies to become gas-deficient, so we will leave aside this curious phenomenon for the moment.

3 RESULTS

We begin by analyzing trends in the $NUV - r$ colours of galaxies as a function of cluster-centric radius. This is a directly observed (as opposed to inferred) quantity that has been found to correlate strongly with the HI gas mass fraction of nearby galaxies (Catinella et al. 2010). In Figure 4, we plot the *difference* in the median $NUV - r$ colour compared to galaxies of the same stellar mass and stellar surface density in the field. Results are plotted as a function of distance from the BCG, scaled to the virial radius of the cluster. The four panels show results for galaxies in different stellar

mass intervals.¹ Black lines show results for all galaxies in a given mass interval, while red and blue curves show results for high and low values of μ_* , respectively. Errors are estimated using a standard bootstrap resampling technique.

In all stellar mass intervals, the difference in $NUV - r$ color increases with decreasing cluster-centric distance. The strength of the effect depends strongly on stellar mass. For galaxies with stellar masses less than $10^{10} M_\odot$, the $NUV - r$ colour reddens by more than 2 magnitudes from the virial radius to the center of the cluster. For galaxies with stellar masses greater than $3 \times 10^{10} M_\odot$, the reddening is only ~ 0.5 magnitudes. The very large differences between the blue and red curves in Figure 4 show that the effect at fixed mass is mainly driven by the dependence of the reddening on surface mass density. We will come back to this point in more detail later.

We now turn to trends in “inferred” HI mass fraction with cluster-centric radius. In the left panel of Figure 5 we plot the difference in the median HI mass fraction with respect to field galaxies of the same stellar mass, as a function of scaled distance from the brightest cluster galaxy (BCG). In the right panel of Figure 5 we show the same plot, except that the HI mass fractions are normalized to field galaxies

¹ For a given stellar mass subsample we use the clusters below the same redshift limit of the galaxy subsample. As a result, for the lowest mass range, $9.6 < \log_{10}(M_*/M_\odot) < 10.0$, only the clusters with $z < 0.04$ is used, while for the other three mass ranges all the clusters with $z < 0.06$ are used.

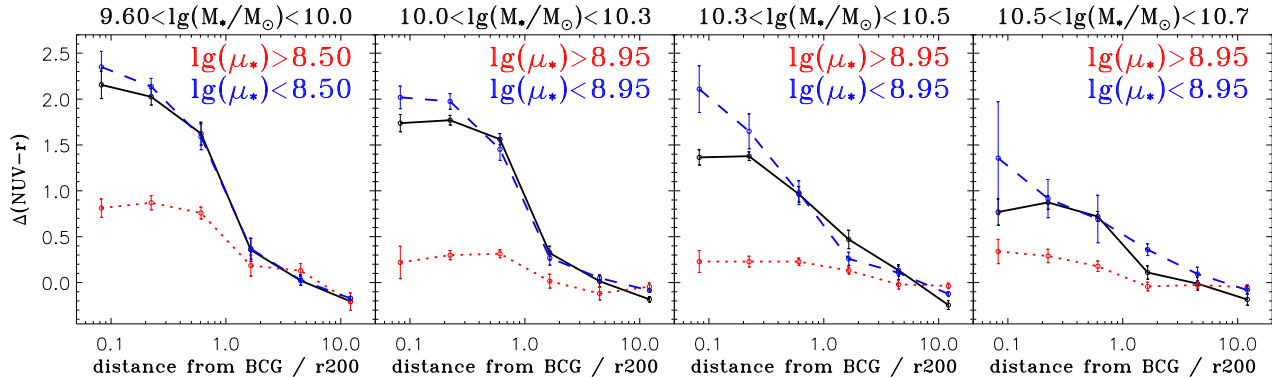


Figure 4. The difference in the median $NUV - r$ colour compared to galaxies of the same stellar mass and stellar surface density in the field. Results are plotted as a function of distance from the BCG, scaled to the virial radius of the cluster. The four panels show results for galaxies in different stellar mass intervals. Black curves show results for all galaxies. Galaxies with higher and lower surface mass density μ_* are shown as red dotted and blue dashed lines (the division points are labelled in each panel). Errors are estimated via bootstrap resampling.

of the same stellar mass and stellar surface mass density, i.e. this is a plot of the HI deficiency parameter defined in the previous section. Figure 5 shows that HI mass fractions drop by a factor of 2-3 at the centers of clusters with respect to “similar” galaxies in the field. The effects are stronger for less massive galaxies. At all masses, the strongest decrease in HI gas fraction occurs just at the virial radius. Interestingly, the decrease in gas fraction with radius is quite shallow in the central region of the cluster.

We now divide the galaxies in each stellar mass interval into two subsets with higher and lower surface mass densities, $\log \mu_*$, and repeat the analysis. The results are shown in Figure 6. The decrease in HI gas content with cluster-centric distance is always stronger for galaxies with low densities. For galaxies with stellar surface densities greater than $10^9 M_\odot \text{ kpc}^{-1}$, there is essentially no change in inferred HI mass fraction with radius.

Figure 7 allows the reader to compare the dependence of HI gas depletion on stellar surface density and on stellar mass at a given clustercentric distance. We plot the mean difference in HI mass fraction with respect to field galaxies of the same stellar mass and stellar surface mass density in the plane of μ_* versus M_* . The four panels show results for galaxies located at different cluster-centric distances. We used a two-dimensional adaptive binning technique to adjust the cell size so that each cell includes a fixed number of galaxies (20, 40, 80 and 80, respectively, for the four cluster-centric distances). It is clear that the decline in HI gas content depends more strongly on stellar surface density than on stellar mass. This is true at all radii within the virial radius of the cluster, but is especially pronounced in the first panel of Figure 7, which shows results for galaxies in the inner cores of the clusters.

3.1 Dependence on halo mass

There are a number of possible reasons why galaxies with low stellar surface densities may lose their gas more efficiently in clusters.

The intracluster medium may exert a drag force on

the gas in galactic disks. If the density of the gas in the disk scales with the density of its stars, then one might expect ram-pressure to act more effectively on galaxies with low stellar surface densities.² Ram-pressure scales with the square of the velocity of the galaxy through the surrounding galaxy, so if this is the main process at work, one would also expect to see it operate more efficiently in clusters with higher velocity dispersions.

Alternatively, encounters between galaxies in groups and clusters may result in stars and other material being pulled out of galaxies. Tidal stripping is most effective when galaxies encounter each other with relative velocities comparable to the internal velocity dispersion of their stars. Tidal stripping is thus not thought to be effective in rich cluster environments, where galaxies are moving with average velocities in excess of 1000 km/s.

In Figure 8, we divide the galaxies in each stellar mass and stellar surface density subsample into two further subsets according to the velocity dispersion of their associated clusters. Our main conclusion is that we do not find any dependence of the gas-radius relation on cluster velocity dispersion, even for low stellar surface mass density galaxies.

4 SUMMARY

In this paper, we have analyzed galaxies in 300 nearby groups and clusters identified in the Sloan Digital Sky Survey using a photometric gas mass indicator that is useful for estimating the degree to which the interstellar medium of a cluster galaxy has been depleted. We study the radial dependence of inferred gas mass fractions for galaxies of different stellar masses and stellar surface densities. Our main results may be summarized as follows.

- The HI mass fraction of galaxies decrease by a factor of 2 – 3 from the outskirts of clusters to their centres. The

² We note that in practice, low density galaxies have larger HI gas mass fractions (Catinella et al. 2010), so this simple assumption is unlikely to hold in detail.

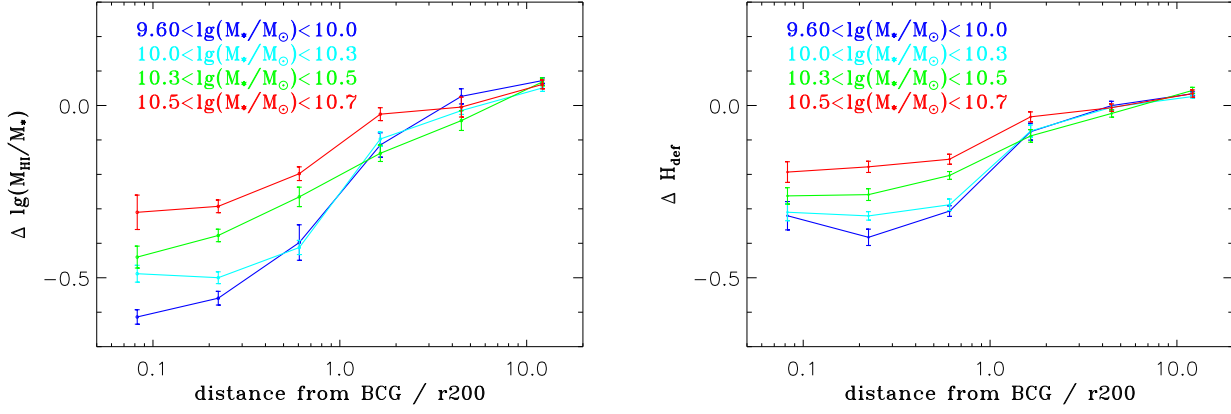


Figure 5. Left panel: The difference in the median H I mass fraction with respect to galaxies of the same stellar mass in the field is plotted as a function of distance from the brightest cluster galaxy. Results are shown for galaxies in different stellar mass intervals as indicated. Right panel: same as the left panel, except that the difference in the median H I deficiency parameter H_{def} with respect to galaxies of the same stellar mass in the field.

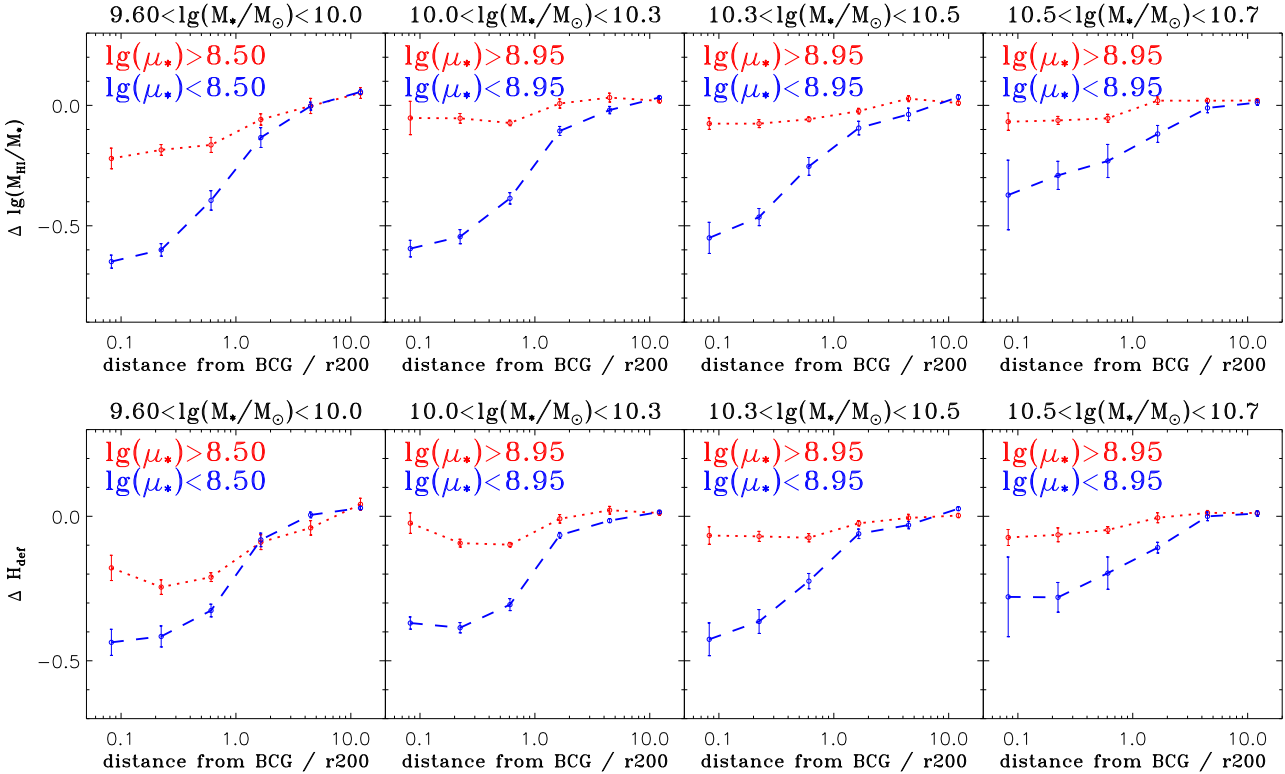


Figure 6. Same as Figure 5, except for each mass interval, the galaxies have been further separated into higher and lower μ_* subsamples, shown as red dotted and blue dashed lines.

decrease in gas fraction is most pronounced around the virial radius and is strongest for low mass galaxies.

- At fixed stellar mass and at fixed clustercentric distance, the depletion of gas in cluster galaxies clearly depends on the stellar surface mass density of the galaxy, in the sense that low density galaxies are more H I deficient.
- An analysis of depletion trends in the two-dimensional plane of stellar mass M_* and stellar mass surface density

μ_* reveals that gas depletion at fixed clustercentric radius is more sensitive to the density of a galaxy than to its mass.

- The gas mass fraction-radius relations exhibit little dependence on the velocity dispersion of the cluster.

We suggest that low density galaxies are more easily depleted of their gas, because they are more easily affected by ram-pressure and/or tidal forces.

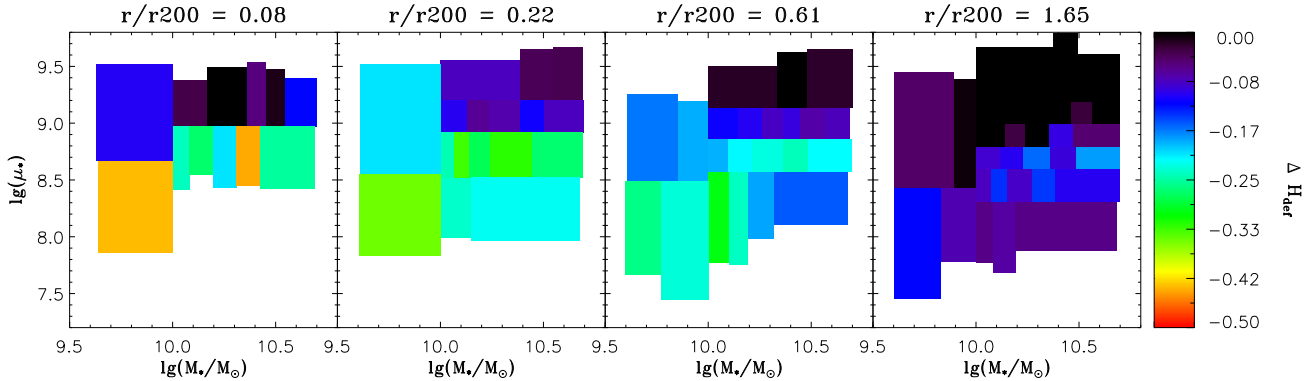


Figure 7. Galaxies at a given range in cluster-centric distance are binned into cells in the 2-dimensional plane of stellar surface mass density versus stellar mass. Each cell is colour-coded according to the mean difference in HI mass fraction with respect to field galaxies of the same stellar mass and surface mass density. Results are shown for four different ranges in cluster-centric distance as indicated on the top of each panel. The cell sizes are adjusted to enclose a fixed number of galaxies, whose value are 20, 40, 80, 80, for the four panels from left to right.

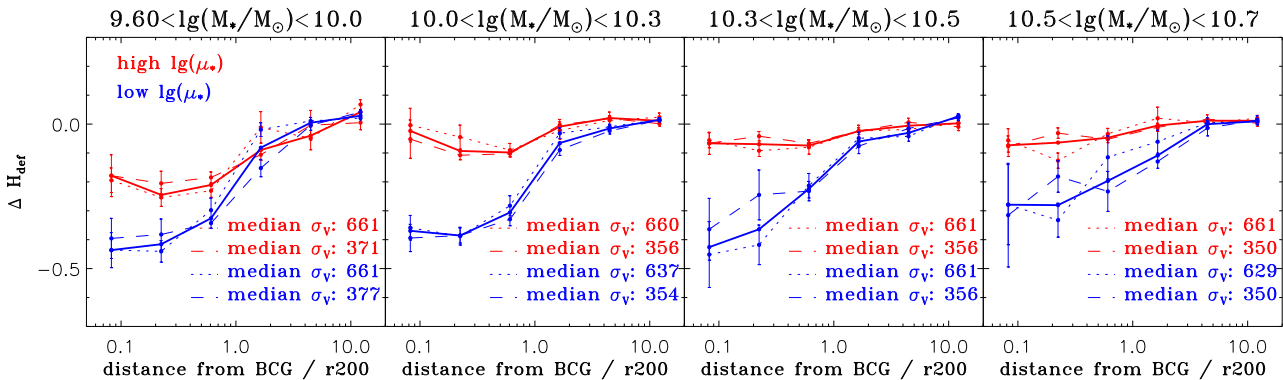


Figure 8. Same as the bottom panel of Figure 6, except that galaxies have been divided into two further subsamples according to the velocity dispersion of their host cluster. A cut at $\sigma = 500$ km/s is applied and the median velocity dispersions clusters hosting the galaxies in the various subsamples are labelled on each panel.

In recent work, Fabello & et al. (2012) compared the environmental density dependence of the atomic gas mass fractions of nearby galaxies with that of their central and global specific star formation rates. For galaxies less massive than $10^{10.5} M_{\odot}$, the authors found both the HI mass fraction and the sSFR to decrease with increasing density, with the HI mass fraction exhibiting stronger trends than the sSFR. This was interpreted as evidence for ram-pressure stripping of atomic gas from the outer disks of low-mass galaxies. The authors also compared their results with predictions from the semi-analytic model (SAM) of Guo et al. (2011). They found the opposite trend in the models: the decline in HI mass fraction with density was weaker than the decline in sSFR. This indicated that the recipe of gas stripping assumed in the current SAMs, in which only the diffuse cold gas surrounding satellite galaxies is stripped (often called “strangulation”), is insufficient, and ram-pressure stripping of the cold interstellar medium is likely to play a significant role.

Li et al. (2012b) studied the bias in the clustering of HI-rich and HI-poor galaxies with respect to galaxies with

normal HI content on scales between 100 kpc and ~ 5 Mpc, and compared the results with predictions from the current semi-analytic models (SAMs) of galaxy formation of Fu et al. (2010) and Guo et al. (2011). They found that, for the HI-deficient population, the strongest bias effects arise when the HI deficiency is defined in comparison to galaxies of the same stellar mass and size. This is not produced by the SAMs, where the quenching of star formation does not depend on the internal structure of galaxies. The authors proposed that the disagreement between the observations and the models might be resolved, if processes such as ram-pressure stripping, which depend on the density of the interstellar medium (ISM), are included in the models.

The results of this paper point in much the same direction. The finding that is somewhat puzzling is that the gas mass fraction-radius relation does not depend significantly on the velocity dispersion of the cluster, as might be expected if ram-pressure stripping is the main process at work in groups and clusters. One possible solution is that *both* tidal and ram-pressure stripping are at work and they act on the galaxy population in such a way as to cancel out any

significant velocity-dispersion dependent effects. There have been recent detailed studies of ram-pressure stripping and tidal interactions in individual galaxy groups with extensive coverage of the X-ray emitting hot gas from *Chandra* observations and detailed HI maps from Very Large Array (VLA) mosaic observations that have indicated that both ram-pressure and tidal stripping can be at work at the same time in a single group (Rasmussen et al. 2012). Next generation X-ray observations from the eROSITA satellite and wide-field HI surveys planned at the Westerbork telescope (APERTIF; Verheijen et al. 2008) and at the Australian SKA Pathfinder telescope (ASKAP) will clarify the relative importance of these processes as a function of dark matter halo mass and location of galaxy within their halos.

ACKNOWLEDGMENTS

WZ and CL thank the Max-Planck Institute for Astrophysics (MPA) for warm hospitality while this work was being completed. This work is supported by the Chinese National Natural Science Foundation grants 10903011 and 11173045, and the CAS/SAFEA International Partnership Program for Creative Research Teams (KJCX2-YW-T23). CL acknowledges the support of the 100 Talents Program of Chinese Academy of Sciences (CAS), Shanghai Pujiang Program (no. 11PJ1411600) and the exchange program between Max Planck Society and CAS. GK thank the Aspen Center for Physics and the NSF Grant #1066293 for hospitality during the writing of this paper. TX acknowledges the support of the LAMOST postdoctoral fellowship.

Funding for the SDSS and SDSS-II has been provided by the Alfred P. Sloan Foundation, the Participating Institutions, the National Science Foundation, the U.S. Department of Energy, the National Aeronautics and Space Administration, the Japanese Monbukagakusho, the Max Planck Society, and the Higher Education Funding Council for England. The SDSS Web Site is <http://www.sdss.org/>.

The SDSS is managed by the Astrophysical Research Consortium for the Participating Institutions. The Participating Institutions are the American Museum of Natural History, Astrophysical Institute Potsdam, University of Basel, University of Cambridge, Case Western Reserve University, University of Chicago, Drexel University, Fermilab, the Institute for Advanced Study, the Japan Participation Group, Johns Hopkins University, the Joint Institute for Nuclear Astrophysics, the Kavli Institute for Particle Astrophysics and Cosmology, the Korean Scientist Group, the Chinese Academy of Sciences (LAMOST), Los Alamos National Laboratory, the Max-Planck-Institute for Astronomy (MPIA), the Max-Planck-Institute for Astrophysics (MPA), New Mexico State University, Ohio State University, University of Pittsburgh, University of Portsmouth, Princeton University, the United States Naval Observatory, and the University of Washington.

REFERENCES

- Berlind A. A., Frieman J., Weinberg D. H., Blanton M. R., Warren M. S., Abazajian K., Scranton R., Hogg D. W., et al., 2006, *ApJS*, 167, 1
- Blanton M. R., Eisenstein D., Hogg D. W., Schlegel D. J., Brinkmann J., 2005, *ApJ*, 629, 143
- Catinella B., Schiminovich D., Kauffmann G., Fabello S., Wang J., Hummels C., Lemonias J., Moran S. M., et al., 2010, *MNRAS*, 403, 683
- Cole S., Aragon-Salamanca A., Frenk C. S., Navarro J. F., Zepf S. E., 1994, *MNRAS*, 271, 781
- Cortese L., Catinella B., Boissier S., Boselli A., Heinis S., 2011, *MNRAS*, 415, 1797
- Diaferio A., Kauffmann G., Balogh M. L., White S. D. M., Schade D., Ellingson E., 2001, *MNRAS*, 323, 999
- Fabello S., et al., 2012, submitted
- Finn R. A., Zaritsky D., McCarthy Jr. D. W., Poggianti B., Rudnick G., Halliday C., Milvang-Jensen B., Pelló R., et al., 2005, *ApJ*, 630, 206
- Font A. S., Bower R. G., McCarthy I. G., Benson A. J., Frenk C. S., Helly J. C., Lacey C. G., Baugh C. M., et al., 2008, *MNRAS*, 389, 1619
- Fu J., Guo Q., Kauffmann G., Krumholz M. R., 2010, *MNRAS*, 409, 515
- Giovanelli R., Haynes M. P., Kent B. R., Perillat P., Sainlonge A., Brosch N., Catinella B., Hoffman G. L., et al., 2005, *AJ*, 130, 2598
- Guo Q., White S., Boylan-Kolchin M., De Lucia G., Kauffmann G., Lemson G., Li C., Springel V., et al., 2011, *MNRAS*, 413, 101
- Jasche J., Kitaura F. S., Li C., Enßlin T. A., 2010, *MNRAS*, 409, 355
- Kannappan S. J., 2004, *ApJL*, 611, L89
- Kauffmann G., White S. D. M., Guiderdoni B., 1993, *MNRAS*, 264, 201
- Kauffmann G., White S. D. M., Heckman T. M., Ménard B., Brinchmann J., Charlot S., Tremonti C., Brinkmann J., 2004, *MNRAS*, 353, 713
- Li C., Jing Y. P., Mao S., Han J., Peng Q., Yang X., Mo H. J., van den Bosch F., 2012a, *ArXiv e-prints*
- Li C., Kauffmann G., Fu J., Wang J., Catinella B., Fabello S., Schiminovich D., Zhang W., 2012b, *ArXiv e-prints*
- Miller C. J., Nichol R. C., Reichart D., Wechsler R. H., Evrard A. E., Annis J., McKay T. A., Bahcall N. A., et al., 2005, *AJ*, 130, 968
- Okamoto T., Nagashima M., 2003, *ApJ*, 587, 500
- Rasmussen J., Bai X.-N., Mulchaey J. S., van Gorkom J. H., Jeltrema T. E., Zabludoff A. I., Wilcots E., Martini P., et al., 2012, *ApJ*, 747, 31
- Schlegel D. J., Finkbeiner D. P., Davis M., 1998, *ApJ*, 500, 525
- Verheijen M. A. W., Oosterloo T. A., van Cappellen W. A., Bakker L., Ivashina M. V., van der Hulst J. M., 2008, in *The Evolution of Galaxies Through the Neutral Hydrogen Window*, Minchin R., Momjian E., eds., Vol. 1035, pp. 265–271
- von der Linden A., Best P. N., Kauffmann G., White S. D. M., 2007, *MNRAS*, 379, 867
- von der Linden A., Wild V., Kauffmann G., White S. D. M., Weinmann S., 2010, *MNRAS*, 404, 1231
- Weinmann S. M., Kauffmann G., van den Bosch F. C., Pasquali A., McIntosh D. H., Mo H., Yang X., Guo Y., 2009, *MNRAS*, 394, 1213
- Weinmann S. M., Kauffmann G., von der Linden A., De Lucia G., 2010, *MNRAS*, 406, 2249
- Weinmann S. M., van den Bosch F. C., Yang X., Mo H. J.,

2006, MNRAS, 366, 2

Wyder T. K., Martin D. C., Schiminovich D., Seibert M.,
Budavári T., Treyer M. A., Barlow T. A., Forster K., et
al., 2007, ApJS, 173, 293

Zhang W., Li C., Kauffmann G., Zou H., Catinella B., Shen
S., Guo Q., Chang R., 2009, MNRAS, 397, 1243